J Solid State Electrochem (1998) 2: 117–122

ORIGINAL PAPER

A.K. Shukla · M.K. Ravikumar · K.S. Gandhi

Direct methanol fuel cells for vehicular applications

Received: 27 May 1997 / Accepted: 25 November 1997

Abstract Dramatic technological advances for the proton exchange membrane fuel cell have focused attention on this technology for motor vehicles. The fuel cell vehicles (FCVs) have the potential to compete with the petroleum-fueled internal combustion engine vehicles (ICEVs) in cost and performance while effectively addressing air quality, energy insecurity, and global warming concerns. Methanol being a liquid can be easily transported and can be supplied from the existing network of oil company distribution sites. Recently, combining improved catalysts with fuel cell engineering, it has been possible to overcome some of the difficulties that have frustrated previous research and development efforts in realizing a commercially viable direct methanol fuel cell. Direct methanol fuel cells (DMFCs) with power densities between 0.2 and 0.4 W/cm^2 at operational temperatures in the range 95–130 °C have been developed. These power densities are sufficient to suggest that stack construction is well worth while. This paper reviews recent advances and technical challenges in the field of DMFCs.

Key words Methanol · Fuel cell · Vehicle · Nafion · Direct methanol fuel cell

Introduction

Deteriorating urban air quality, growing dependence on insecure energy sources and global warming are major challenges forcing reexamination of petroleum-fueled internal combustion engine vehicles (ICEVs) as the basis for road transportation throughout the world. To meet the air quality goals in the face of continuing growth in transport fuel demand, tailpipe emission standards have been progressively tightened in many countries. But tailpipe emission control devices have been getting even more complicated, expensive, and difficult to maintain. The spectre of energy insecurity that haunted energy planners in the 1970s is re-emerging. Energy input dependence is rising, and the share of world oil production coming from the middle east is growing. While soft oil prices may persist for a few years, supplies will eventually tighten because of rapidly growing transport energy demand, more so in the developing countries. The deleterious effect of oil imports on our economy is too well known to be recounted here [1].

Methanol and hydrogen derived from bio-mass offer the potential for making major contributions to transport fuel requirements by addressing competitively all of these challenges, especially when used in fuel cell vehicles (FCVs). In a fuel cell, the chemical energy of a fuel is converted directly into electricity without first burning the fuel to generate heat to run a heat engine. Since fuel cells operate without a thermal cycle, they offer a quantum leap in energy conversion efficiency and virtual elimination of air pollution without the use of emission control devices [2].

Research toward the development of fuel cells for vehicular application has primarily relied on the use of proton-exchange membranes such as Nafion as the electrolyte. Figure 1 shows the basic design of a typical H_2-O_2 fuel cell employing Nafion electrolyte. The key components of the fuel cell are an anode to which hydrogen is supplied, a cathode to which oxygen is supplied and the Nafion electrolyte which permits the flow of protons between the anode and cathode. Two chemical reactions take place at the same time. At the anode, gaseous hydrogen fuel undergoes oxidation following the reaction: $H_2 \rightarrow 2H^+ + 2e^-(E_a = 0.0\ V\ \text{vs SHE})$, while, at the cathode, gaseous oxygen is reduced to

Presented at the 3rd Indo-German Seminar on 'Modern Aspects of Electrochemistry', 26 September – 1 October 1996, Bangalore, India

A.K. Shukla (✉) · M.K. Ravikumar
Solid State and Structural Chemistry Unit,
Indian Institute of Science, Bangalore-560 012, India

K.S. Gandhi
Department of Chemical Engineering,
Indian Institute of Science, Bangalore-560 012, India

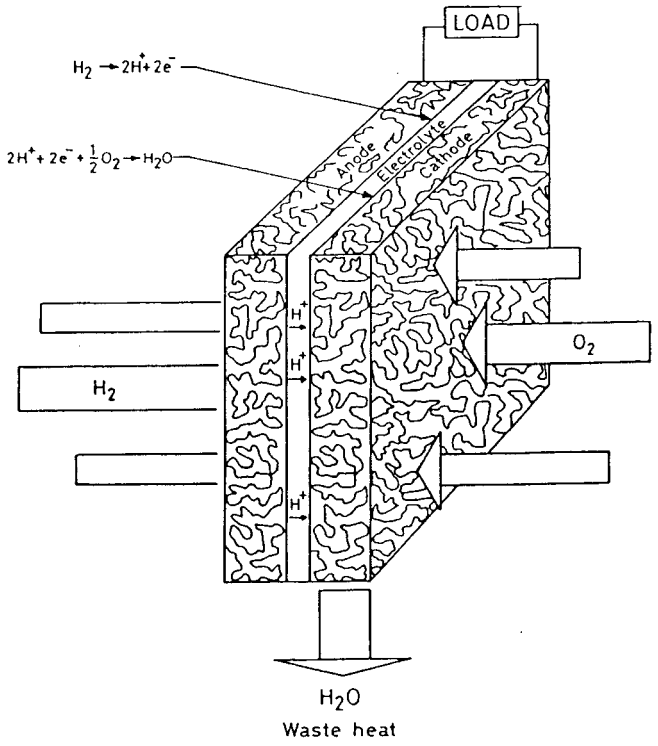

Fig. 1 A solid-polymer electrolyte hydrogen-oxygen fuel cell

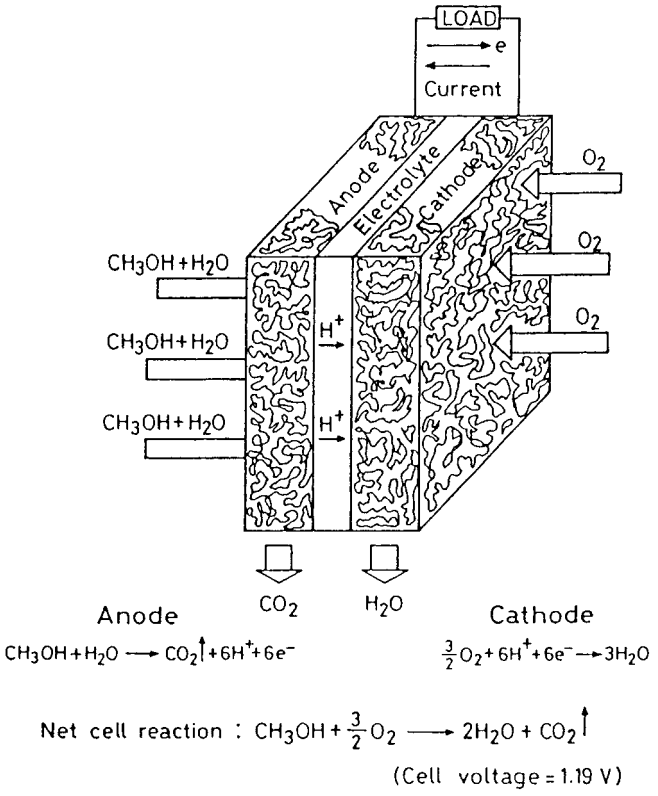

Fig. 2 A solid-polymer electrolyte direct methanol fuel cell

produce water following the reaction: $2H^+ + 2e^- + \frac{1}{2}O_2 \rightarrow H_2O$ ($E_c = 1.23$ V vs SHE). Accordingly, the net cell reaction is: $H_2 + \frac{1}{2}O_2 \rightarrow H_2O$ ($E_{cell} = E_c - E_a = 1.23$ V) [3–6]. When the cell is connected to an external circuit (load), the excess electrons flow from the anode through the circuit and back to the cathode. As the electrons move through the circuit, they lose energy. This energy may be used to create heat or light as in an electrical heater or light bulb, or to do work as in a motor. The flow of electrons results in a current, and by convention the direction of flow of current is taken as opposite to the direction of flow of electrons. The energy difference per unit charge while electrons flow through the circuit is called voltage. The product of the current and voltage is the power delivered to the circuit.

The performance of the H_2-O_2 proton-exchange membrane electrolyte fuel cell, particularly under a few bar pressure, is quite remarkable where power densities in excess of $1\,Wcm^{-2}$ have been achieved [7]. These performances should not, however, disguise the fact that if the application of such fuel cells to transport is considered, particularly if methanol is used as the fuel and the reformer is used, there are several additional sources of loss. Operation of the fuel cell at 5 bar leads to an air-compressor loss of ca. 12% of stack output, and reformer losses of 10–15% based on the heating value of the input methanol fuel are to be expected. Further losses to ancillary units and in power converters, etc., can lead to overall power efficiencies from methanol chemical energy to wheels of ca. 15%. Hydrogen can as well can be carried on the vehicle (a) as liquefied hydrogen, (b) as absorbed gas within certain alloys, and (c) as compressed gas. The last option is favoured at present, though it has obvious safety hazards. Ballard have recently designed and constructed a bus that uses compressed hydrogen in cylinders as the fuel, and have been testing this for city driving in Vancouver [8]. By contrast, methanol being a liquid can be easily transported and can be supplied from the current network of oil company distribution sites.

In a fuel cell, methanol can be directly oxidized to carbon dioxide and water at the anode following the reaction [9]:

$$CH_3OH + H_2O \rightarrow CO_2\uparrow + 6H^+ + 6e^- \quad (E_a = 0.04 \text{ V vs SHE}) \tag{1}$$

The reduction of oxygen takes place at the cathode:

$$\tfrac{3}{2}O_2 + 6H^+ + 6e^- \rightarrow 3H_2O \quad (E_c = 1.23 \text{ V vs SHE}) \tag{2}$$

Accordingly, the net cell reaction is:

$$CH_3OH + \tfrac{3}{2}O_2 \rightarrow CO_2\uparrow + 2H_2O \quad (E_{cell} = E_c - E_a = 1.19 \text{ V}) \tag{3}$$

A direct methanol fuel cell (DMFC) with a Nafion electrolyte is shown schematically in Fig. 2. The fundamental limitation in the practical realization of such a DMFC has been the existence of electrochemical losses at both the anode and cathode leading to poor overall

conversion efficiencies. One of the reasons is the methanol crossover via the electrolyte to the cathodes. Besides, the direct oxidation of methanol to carbon dioxide at platinum-based catalytic electrodes requires six electrons and there is little probability of all being transferred simultaneously. Moreover, it is not possible to devise a mechanistic route for methanol oxidation solely involving low-energy solution intermediates, and low-energy routes through CO_2 require surface-bound intermediates. In the literature, considerable effort has been expended in studying the details of this mechanism, and in understanding the role of promoters such as ruthenium, which has led to rapid advances in catalyst performance [10–14].

Electrocatalysis and electrode performance

The performance of a fuel cell is represented by the current density vs voltage (or polarization) curve shown in Fig. 3. Ideally a single DMFC could produce 1.19 V (d.c). In practice, however, it produces voltage outputs that are somewhat less than the ideal value, which decreases with increasing load current-densities, as shown in Fig. 3. The losses or reduction in voltage from the ideal value are referred to as polarization or over-potential. The polarization curve comprises three distinct regions. The first region (I) belongs to the voltage loss at low currents, is due to the interface resistance, and is termed the activation polarization region. The second region (II) is characterized by a linear drop with increasing current, is due to the intrinsic ohmic resistance, and is termed the ohmic polarization region. The third region (III) is termed the diffusion-limited or concentration-polarization region and is represented by a final additional drop at high currents arising because of the depletion of acceptors at the interface for the transitory species [15].

Polarization losses in the activation polarization regime are usually circumvented by the use of an active catalyst. To expand further, for an electrochemical process [16],

$$\mathrm{O} + n\mathrm{e}^- \underset{k_\mathrm{b}}{\overset{k_\mathrm{f}}{\rightleftharpoons}} \mathrm{R} \tag{4}$$

the net rate of the reaction is,

$$\frac{I}{nFA} = k_\mathrm{f} C_\mathrm{O} - k_\mathrm{b} C_\mathrm{R} \tag{5}$$

where k_f and k_b are rate constants for the forward and backward reactions, respectively, C_O and C_R are concentrations of the O and R species, A is the area of the electrode, F is the faraday constant, $k_\mathrm{f} = k^\mathrm{o}\mathrm{e}^{-\alpha n f \eta}$ and $k_\mathrm{b} = k^\mathrm{o}\mathrm{e}^{\beta n f \eta}$, k^o is the standard rate constant, η is the associated polarization, and α and β are energy-transfer coefficients that are indicators of the form of the reaction barrier. Even though the net reaction is zero at equilibrium, one still envisages balanced faradaic activity

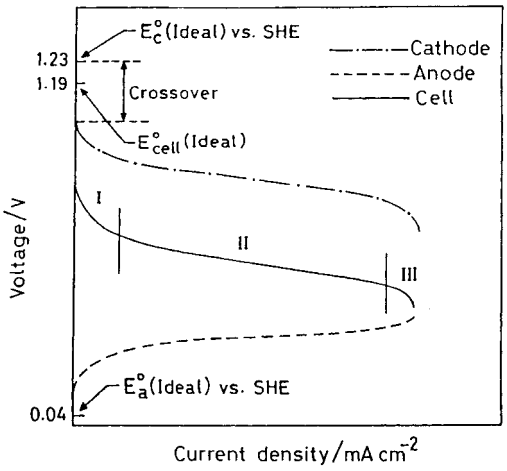

Fig. 3 The polarization curves for a direct methanol fuel cell and its constituent electrodes

that can be expressed in terms of the exchange current, I_o, and is equal to $nFAk^\mathrm{o}C$, where $C_\mathrm{O} = C_\mathrm{R} = C$.

If the solution is well stirred or the current is kept so low that the surface concentration does not differ appreciably from the bulk values, then Eq. 5 takes the form

$$\frac{I}{I_\mathrm{o}} = \mathrm{e}^{-\alpha n f \eta} - \mathrm{e}^{\beta n f \eta} \tag{6}$$

Equation 6 is called the Butler-Volmer equation. The first and second terms on the right-hand side of Eq. 6 represent the cathodic and anodic components, respectively. At larger exchange currents I_o tends to ∞, making $\frac{I}{I_\mathrm{o}} \to 0$.
Consequently, Eq. 6 takes the form,

$$\mathrm{e}^{-\alpha n f \eta} = \mathrm{e}^{\beta n f \eta} \tag{7}$$

In Eq. 7 α, β, n and f are not equal to zero, and hence, at I_o tending to ∞, η would tend to 0. Therefore, the purpose of employing a catalyst is to make $\eta \to 0$ at low current densities.

The most effective and common catalyst employed with fuel cells is platinum. Because of the high work function of platinum, the kinetic window for the electron transfer can be varied widely both for anodic and cathodic reactions to proceed favourably. But platinum is not particularly active for methanol oxidation. Platinum poisons easily, and cell performance degrades with time both at low and high over-potentials. In the literature, the mechanism of methanol oxidation on platinum particles remains controversial, a fact that makes rational catalyst design substantially difficult. It is widely accepted that methanol undergoes chemisorption onto the platinum surface by stepwise stripping of the three methyl-group protons as follows [17]:

$$\mathrm{CH_3OH} \xrightarrow{k_1} \mathrm{Pt{-}CH_2OH} + \mathrm{H^+} + \mathrm{e^-} \tag{8}$$

$$\mathrm{Pt{-}CH_2OH} \xrightarrow{k_2} \mathrm{Pt_2{=}CHOH} + \mathrm{H^+} + \mathrm{e^-} \tag{9}$$

$$Pt_2{=}CHOH \xrightarrow{k_3} Pt_3COH + H^+ + e^- \quad (10)$$

where $k_1 < k_2 < k_3$ makes Pt_3COH a predominant species. Further oxidation of the intermediate Pt_3COH to linearly bonded Pt_3CO is known to occur, although whether there is a true intermediate or simply a surface poison is a matter of debate. Oxidation of either Pt_3COH or Pt_3CO is thought to take place by absorbed OH species. At potentials (below 450 mV vs SHE) the surface of platinum is heavily covered with CO_{ads} [18]. Although the rate of chemisorption of methanol is certainly fast enough to replace any CO_{ads} that might be lost by further oxidation, turnover of the surface CO species is insignificant. The most likely mechanism is then that water adsorbs on vacant sites close to active sites, to which it can migrate and turnover to CO_2. These steps can be written as:

$$Pt_3COH \rightarrow Pt_3CO + H^+ + e^- \quad (11)$$

$$Pt_3CO + H_2O \rightarrow Pt_3 + CO_2 \uparrow + 2H^+ + 2e^- \quad (12)$$

The evidence for the presence of active sites comes from the observation that the activity of Pt/C catalyst is critically dependent on the strength of the reducing agent [19].

Studies on promotion by co-reducing platinum with other noble metals suggested that ruthenium markedly increases the catalytic activity of platinum at all potentials but particularly in the high-potential region, the optimum composition being 50Pt-50Ru. Methanol oxidation on Pt-Ru particles proceeds through the following steps [20].

$$3Pt + CH_3OH \rightarrow Pt_3COH + 3H^+ + 3e^- \quad (13)$$

$$Ru + H_2O \rightarrow RuOH + H^+ + e^- \quad (14)$$

$$RuOH \rightarrow RuO + H^+ + e^- \quad (15)$$

$$RuO + Pt_3COH \rightarrow Ru{+}3Pt + CO_2\uparrow + H^+ + e^- \quad (16)$$

Efforts have also been expended to explore Pt-M alloys where M can be leached. The best known of these is Pt-Sn [21]. Optimization of this catalyst showed that the optimum ratio of Pt-Sn lies in the region 1:1–1:2, which coincides with the formation of Pt-Sn (hexagonal) and $PtSn_2$ (cubic) alloys [22]. It is known that Sn leaches from these alloys and the promotion is seen in the low-potential regions. The methanol oxidation on Pt-Sn alloys can be envisaged as follows:

$$\begin{array}{l} Sn \\ | \\ Pt \end{array} + CH_3OH \rightarrow \begin{array}{l} Sn \\ | \\ Pt{-}CHO \end{array} + 3H^+ + 3e^- \quad (17)$$

$$\begin{array}{l} Sn \\ | \\ Pt{-}CHO \end{array} + H_2O \rightarrow \begin{array}{l} Sn\text{-}OH \\ | \\ Pt{-}CHO \end{array} + H^+ + e^- \quad (18)$$

$$\begin{array}{l} Sn{-}OH \\ | \\ Pt{-}CHO \end{array} \rightarrow \begin{array}{l} Sn{-}OH \\ | \\ Pt{-}CO \end{array} + H^+ + e^- \quad (19)$$

$$\begin{array}{l} Sn{-}OH \\ | \\ Pt{-}CO \end{array} \rightarrow \begin{array}{l} Sn \\ | \\ Pt \end{array} + CO_2 \uparrow + H^+ + e^- \quad (20)$$

Further studies on this family of alloy catalysts have been carried out on Pt-Cr, Pt-Fe and Pt-Cu alloys. These studies suggested that more active catalysts might be made by combining two metals that promote in different ways. The obvious pair was Sn and Ru, but severe difficulties were experienced with this. Since Sn and Ru are quite miscible, formation of Pt-Sn alloy led to expulsion of Ru. Recently, however, the ternary system Pt-Ru-Sn has proved to be extremely active [18].

In an electrochemical cell, the operating voltages are necessarily low, so high power (IV) requires a high current. A low internal-loss (I^2R) requires in turn a small resistance (R) of $L/\sigma A$, where L is the thickness of the electrolyte separator, A its area and σ its conductivity. For low R, in addition to large σ, it is necessary to have a large-area-thin-membrane electrolyte to circumvent ohmic polarization. Usage of Nafion, a perfluorosulphonic acid polymer electrolyte with high H^+-ion conductivity, is considered a major step forward in the development of polymer electrolyte membrane fuel cells. Nafion, being water-insoluble, has no volume management problems and automatically rejects pure product water, giving a benign corrosion environment in the fuel cell. Polymer-electrolyte-membrane fuel cells employing Nafion as the electrolyte cannot be operated at low humidity because they become dry and non-conducting. The practical operating temperature limit is about 90 °C unless very high partial vapour pressures are used for humidification. Nafion is also permeable to methanol, and hence efforts are being expended to reduce methanol crossover in DMFCs using it. For example, copolymers of perfluorodimethyldioxole and tetrafluoroethylene (PDD-TFE) are compatible with Nafion solution, can be fabricated into ultra-thin membranes, and have good methanol crossover resistance [23].

Concentration polarization represents the energy losses associated with mass-transport effects. In particular, the performance of an electrode may be inhibited by the inability of the reactants to diffuse to products or products to diffuse away from the reaction site. In fact, at some current value, namely the limiting current value, i_l, a situation will be reached wherein the current will be completely limited by the diffusion process. Taking the diffusion constant for the reacting species as D, C_b as the bulk concentration, C_e as the concentration at the electrode surface, and δ as the diffusion-layer thickness, the rate of flow can be written as [16]

$$\frac{I}{nF} = \frac{AD(C_b - C_e)}{\delta} \quad (21)$$

$$\frac{I}{A} = i = \frac{DnF(C_b - C_e)}{\delta} \tag{22}$$

At $i \to i_l, C_e \to 0$ with $\delta \to \delta_l$. Accordingly,

$$i_l = \frac{DnFC_b}{\delta_l} \tag{23}$$

Dividing Eq. 22 by Eq. 23, we have

$$\frac{i}{i_l} = \left(\frac{C_b - C_e}{C_b}\right)\frac{\delta_l}{\delta} \tag{24}$$

when $\delta \to \delta_l$, Eq. 24 can be written as

$$i = \left(\frac{C_b - c_e}{C_b}\right) i_l \tag{25}$$

From the Nernst relationship, we can express

$$\eta = \frac{RT}{nF} \ln \frac{C_e}{C_b} \tag{26}$$

Substituting from Eq. 25 in Eq. 26, we have

$$\eta = \frac{RT}{nF} \ln\left(1 - \frac{i}{i_l}\right) \tag{27}$$

From Eq. 27 it is obvious that as i_l tends to ∞, η would tend to 0.

In order to increase i_l, the reacting species have to be made available to the electrode surface even at very high operational currents.

Fuel cell electrodes demand specifically designed electrode structures and electrocatalyst morphologies. The development of materials and production technologies of electrocatalysts, electrodes and cells is far from finished. The issue of fuel cell development today is more a matter of materials science than of fundamental electrochemical research. In the context of electrode morphology, optimization modelling of electrode performance is an indispensable tool [24].

Recent developments in DMFCs

The rapidity of progress in the development of DMFCs within the last two years has been astonishing. Proton-exchange-membrane-electrolyte DMFCs with (a) vapour and (b) liquid-feed configurations have been constructed and tested [25–29]. The current-voltage characteristics reported for vapour-feed DMFC are shown in Fig. 4. The data show that a current density of 300 mA cm^{-2} can be derived at a cell voltage of 550 mV, which is equivalent to a power density of $\sim$0.16 W cm^{-2} at the operational temperature of $\sim$90 °C.

The schematics of a liquid-feed DMFC is shown in Fig. 5. This configuration is more attractive since it avoids the evaporator. The current-voltage characteristics reported [28] for the liquid-feed DMFC is shown in Fig. 6. The data show that a power density of $\sim$0.18 W cm^{-2} can be derived from this type of DMFC

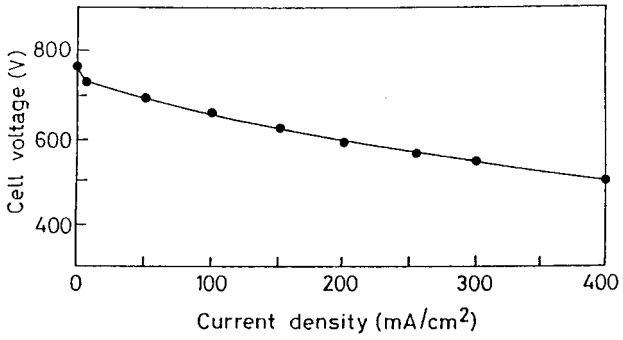

Fig. 4 Galvanostatic polarization data of vapour-feed DMFC at 95 °C with 2 bar O_2 pressure ([25])

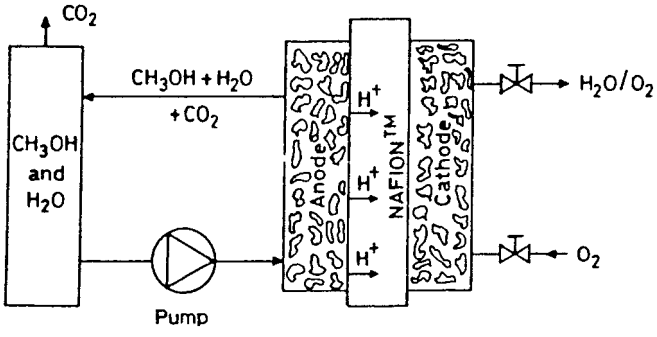

Fig. 5 A solid-polymer electrolyte (Nafion) liquid-feed DMFC (from [28])

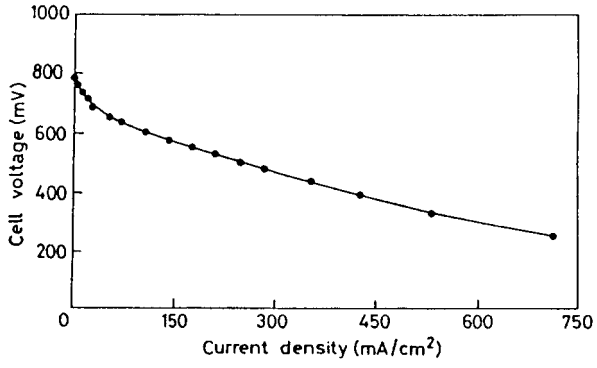

Fig. 6 Galvanostatic polarization data of the liquid-feed DMFC (from [28])

at an operational temperature of $\sim$90 °C. The endurance test carried out on this DMFC suggested that the cell can be operated continuously for $\sim$100 h with little deterioration (Fig. 7). We have extended these studies to stack construction. The performance data for a 5 W DMFC stack at an operational temperature of 90 °C are shown in Fig. 8 [29]. Recently, it has been shown that power densities as high as 0.4 Wcm^{-2} can be achieved by operating the cell at about 130 °C [27].

There is no reason to believe that the cell engineering is fully optimized, and further improvements are highly likely. Nevertheless, these power densities are sufficient to suggest that stack construction is well worth while. A

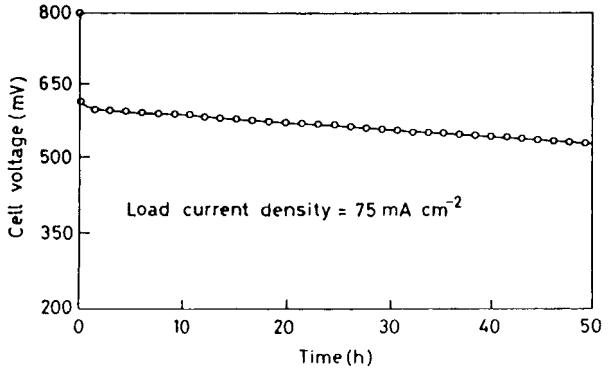

Fig. 7 Endurance test of the liquid-feed DMFC (from [28])

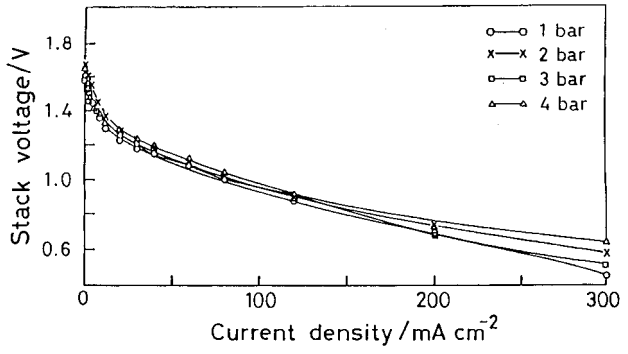

Fig. 8 Performance characteristics of the 5 W liquid-feed DMFC stack at 90 °C at various oxygen gas pressures ([29])

fuel cell of this type, if perfected, will have many attractions for FCVs. The energy density of methanol fuel in such a fuel cell would be about 6 kWh/kg. Methanol-fueled FCVs will be about $2\frac{1}{2}$ times more energy efficient than ICEVs. For hydrogen-fueled FCVs, air pollution from the vehicle would be zero, while for methanol fueled FCVs these emissions would be non-zero but minuscule as compared to ICEVs.

The problems that remain to be solved are: (1) to find electrocatalysts that would (a) enhance the electrode kinetics of methanol oxidation, and (b) minimize the poisoning caused by strong adsorption of CO-type intermediates, (2) find electrocatalysts for oxygen reduction which are not depolarized by the methanol crossover from the anode to the cathode via the membrane by optimizing the structure of the electrodes and the operating conditions or by finding membranes which inhibit the methanol transport, and (3) the engineering design and construction of the electrochemical multistack.

Conclusions

For transportation, the proton-exchange membrane DMFCs offer the greatest advantage in terms of environmental factors, but there remains much developmental work to do. Nevertheless, the overall picture is a positive one, and indeed the extraordinary progress made over the past few years has placed DMFCs firmly on energy-forcasting panels the world over.

References

1. Williams RH, Larson ED, Katofsky RE, Chen J (1995) Energy for Sustainable Development 1: 18
2. Liebhafsky HA, Cairns EJ (1968) Fuel Cells and Fuel Batteries – A guide to their research and development. Wiley, New York
3. Appleby AJ, Foulkes FR (1989) Fuel Cell HandBook. Von Nostrand Reinhold, New York
4. Appleby AJ (1995) In: Bisic A, Boots S (eds) Encyclopedia of Energy Technology and the Environment vol 2. Wiley, New York
5. Berger C (ed) (1968) Handbook of Fuel Cell Technology. Prentice-Hall, Engelwood Cliffs, New Jersey
6. Vielstich W (1970) Fuel Cells, translated into English. Wiley-Interscience, London
7. Murphy OJ, Hitchens GD, Manko DJ (1994) J Power Sources, 47: 353
8. Prater KB (1994) J Power Sources, 51: 129
9. Bockris J O'M, Srinivasan S (1969) Fuel Cells: Their Electrochemistry. McGraw-Hill, New York
10. McNicol BD (1981) J Electroanal Chem 118: 71
11. Parsons R, Vander Noot T (1988) J Electroanal Chem 257: 9
12. Hamnett A, Weeks SA, Kennedy BJ, Troughton G, Christensen PA (1990) Ber Bunsenges Phys Chem 94: 1014
13. Leger J.M, Lamy C (1990) Ber Bunsenges Phys Chem 94: 1021
14. Iwasita-Vielstich T (1991) In: Gerischer H, Tobais CW (eds) Advanced Electrochemical Engineering (New series) 1: 127
15. Ficket AP (1984) In: Linden D (ed) Handbook of batteries and fuel cells. McGraw-Hill
16. Bard AJ, Faulkner LR (1980) Electrochemical methods: fundamentals and applications. Wiley, New York
17. Bagotsky VS, Vassilev Yu. B (1977) J Electroanal Chem 81: 229
18. Hamnett A, Troughton GL (1992) Chem Ind 480
19. Shukla AK, Ramesh KV, Manoharan R, Sarode PR, Vasudevan S (1985) Ber Bunsenges Phys Chem 89: 1261
20. Goodenough JB, Manoharan R, Shukla AK, Ramesh KV (1989) Chem Mater 1: 391
21. Watanabe M, Furuuchi Y, Motoo S (1985) J Electroanal Chem 191: 367
22. Aricó AS, Antonucci V, Girodano N, Shukla AK, Ravikumar MK, Roy A, Barman SR, Sarma DD (1994) J Power Sources 50: 295
23. Agency Proposal No. 10.02-1762, SBIR/STTR (1996)
24. Wendt H, Brenscheidt T, Fischer A (1996) Phil Trans R Soc Lond A 354: 1627
25. Shukla AK, Christensen PA, Hamnett A, Hogarth MP (1995) J Power Sources 55: 89
26. Surampudi S, Narayanan SR, Vamos E, Frank H, Halpert G, Laconti A, Kosek J, Surya Prakash GK, Olah GA (1994) J Power Sources 47: 377
27. Ren X, Wilson MS, Gottesfeld S (1996) J Electrochem Soc 143: L12
28. Ravikumar MK, Shukla AK (1996) J. Electrochem Soc 143: 2601
29. Ravikumar MK (1996) Ph.D. thesis. Indian Institute of Science, India